A fast and robust maximum power point tracker for photovoltaic systems using variable structure control approach

Faramarz Karbakhsh Ravari
Electrical Engineering Department
Faculty of Engineering, Ferdowsi University of Mashhad
Mashhad, Iran
fa.karbakhshravari@stu-mail.um.ac.ir

H. Abootorabi Zarchi
Electrical Engineering Department
Faculty of Engineering, Ferdowsi University of Mashhad
Mashhad, Iran
abootorabi@um.ac.ir

***Abstract*—This paper presents a fast and robust maximum power point tracking scheme for photovoltaic (PV) generators. The fast dynamics is achieved by a sliding mode-plus-PI controller with a new optimal switching surface based on P-I characteristics of PV panels. The proposed controller is able to reduce the output power fluctuations during steady-state behavior while the fast response and robustness merits of the sliding mode controller are preserved. In response to a sudden change in radiation and temperature, the validity and capability of the method are verified by a grid-tied two switch flyback solar micro inverter simulation results. This topology mitigates the problem of high-voltage transients at switch turn off which commonly exists in single switch flyback inverters.**

Keywords— Photovoltaic systems, sliding mode control, maximum power point tracking, robust and fast approach, two-switch flyback topology

I. INTRODUCTION

Despite the relatively high cost of solar modules, photovoltaic (PV) power system has been commercialized all over the world due to its long term economic prospects and the concerns over the environment [1]. The PV generator (PVG) exhibits nonlinear *I–V* and *P–V* characteristic curves. The maximum power produced depends on both irradiance and temperature. Since the conversion efficiency of PV arrays is very low, it requires maximum power point tracking (MPPT) control schemes. The MPPT is the automatic control algorithm to adjust the power interfaces and achieve the greatest possible power harvest, during variations of insolation level, temperature, and photovoltaic module characteristics. The purpose of the MPPT is to adjust the solar panel operating set point close to the MPP under changing atmospheric conditions.

Typically, the MPPT power stage is executed by means of a dc-dc switching converter at the front end, most commonly pulse width modulated (PWM). In addition, the MPPT must include a self-tuning mechanism which governs the power stage and drives the system to operate at the MPPT (eventually through the converters duty cycle) [2], [3]. Many MPPT schemes have been proposed [4], some exhibit better performance in steady state conditions [4], [5], while others are superior during transitions [6]–[15]. The perturb and observe (P&O) and the Hill-Climbing algorithms are probably those most widely used. The MPPT algorithm operation principle is quite similar for both, the voltage and current at the power stage input are sensed and the power is calculated; then, the MPPT is sought iteratively. These algorithms imply a tradeoff in choosing the increment value by which the controlled parameter, such as duty cycle or reference voltage, is adjusted; small values decrease the losses in steady state due to small perturbations around the MPP, while large values improve the dynamic behavior in situations involving sudden changes in radiation levels or load characteristics, especially in portable applications [6]–[8]. Recently, effort was made to execute MPPT algorithms with adaptive step size. Sophisticated algorithms present two main drawbacks: increased computational load which may require costly hardware and a slow dynamic response which is an intrinsic limitation resulting from the iterative search nature requiring successive sampling of voltage and current. The time intervals between algorithm iterations should be short to satisfy faster tracking, but on the other hand they must be longer than the settling time of the PV current and voltage for reliable signal measurement. Therefore, the analysis of a PV system dynamics is required to determine the P&O time intervals and controller parameters [9].

Employing a converter that is optimized for interfacing with the PVG has a significant effect on the dynamics of the system [10]–[13].

Based on the PV module characteristics, the MPP locus may be approximated by a linear function [11], [12]. Therefore, a linear controller was designed which drives the PVG to its approximate MPP situation. Hardware implemented, this action is performed much faster than the MPPT algorithm. Then, the MPPT algorithm may apply small steps to drive the operation point to the exact MPP.

Variable Structure Control (VSC) or sliding mode control (SMC) is an effective, high frequency switching control for nonlinear systems with uncertainties. It features simple implementation, disturbance rejection, strong robustness and fast responses. Since switched mode converters are, by their nature, switching devices, it is worth considering VSC as a solution for generating discontinuous control laws [16-18]. In [18] a sliding-mode based MPPT method was introduced. In comparison to PWM based MPPTs, convergence to maximum

power is accelerated by an order of magnitude, in response to variations in radiation. This is accomplished by an optimal selection of the switching surface. In addition, the sliding-mode guarantees stability all across the photovoltaic curve.

The main drawback of the conventional flyback inverter is high voltage and current stresses which suffer the switches. At switch turn-off, high-voltage transients are caused by the resonant behavior of the transformer leakage inductance and the transistor output capacitance, resulting in a high-voltage stress which leads to high conduction and switching losses. A solution to remove ringing in the single-switch flyback converter is the two-switch flyback converter. The maximum voltage stress of the switch in a two-switch flyback converter is limited only to the DC input voltage V_{in}, reducing the switching and conduction losses. Operation of two switch flyback inverter in photovoltaic ac module systems hasn't been much analyzed. In [19] a two stage flyback micro-inverter has been proposed. Existence of one additional high frequency power conversion stage has a negative effect on the overall conversion efficiency. In [20] a flyback micro inverter linked to a three phase utility grid has been introduced which is not much applicable in ac module systems because almost all of these systems are single phase grid connected.

In this paper, a sliding mode-plus-PI controller is employed. It consists of a switching component and a linear PI regulator for current control. The proposed controller takes advantage of the best features of linear control, smooth operation, and of VSC, robustness to perturbations. During transients, the linear component is dominant, and the PI gains are selected so as the linear control realizes the desired dynamic response. Moreover, a new adaptive switching surface is introduced by a linear combination of the PVG current and power, regarding irradiance and temperature simultaneously.

This paper is organized as follows. Section II presents the principles of the proposed MPPT with new switching surface. Section III suggests a liner VSC method for high tracking efficiency for a maximum power point algorithm with fine step. Section IV presents the proposed two switch flyback inverter topology. Finally, in order to verify the performance of the proposed MPPT algorithm, simulation results are presented in section V.

II. PRINCIPLES OF THE PROPOSED MPPT METHOD

A. Proposed Switching Surface

The PV generators exhibit nonlinear *I–V* and *P–V* characteristic curves. The maximum power produced depends on both irradiance and temperature. Reference [18] with the aid of *I-V* curves of PVG's, defines a switching surface that satisfies MPPT regarding only irradiance. The proposed surface in [18] is:

$$S(V, i) = a\, i - b\, V + ref = 0 \tag{1}$$

Where V and i are PVG output voltage and current, and a, b, and ref define the switching surface. Fig. 1, shows the proposed surface. The effect of temperature is not considered in this switching surface; moreover, it requires a considerable value of ref as is depicted in Fig. 1.

Considering *P-I* curves of PVG's, a new optimal switching surface is introduced that satisfies MPPT regarding both irradiance and temperature simultaneously. With respect to Fig. 2, which depicts the *P-I* PVG curve and the new proposed switching surface, in the case of changes in irradiance, the proposed switching surface is given by (2):

$$S(P, i) = P - k_1\, i + ref = 0 \tag{2}$$

Where P and i are PVG output power and current respectively, and k_1 and ref define the switching surface.

Through simulation of a variety of PV panels made by different manufactures, using a PV model given in [21], it is shown that in the case of *P-I* curves, one may notice that defining a switching surface without considering intercept does not lead to unbearable power loss. For brevity, the analysis results have been reported just for one PV panel in Table I. In Table I, I_{mpp} and P_{mpp} are the current and the output power of the noticed PVG in the maximum power point. $P_{mpp,1}$ is the estimated power by the surface S_1, and $P_{mpp,2}$ is the estimated power by the surface S_2. The surface S_1 is obtained by applying minimum squared error (MSE) method to the set of MPP's which corresponds to the different levels of radiation, and S_2 is the surface which links the origin to the MPP that corresponds to the standard test condition (STC). E_{rror1} and E_{rror2} are defined as follow:

$$E_{rror1} = \frac{P_{mpp} - P_{mpp,1}}{P_{mpp}} \times 100 \tag{3}$$

$$E_{rror2} = \frac{P_{mpp} - P_{mpp,2}}{P_{mpp}} \times 100 \tag{4}$$

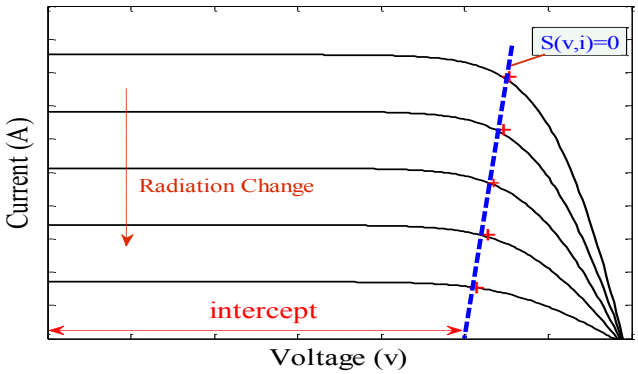

Fig. 1. *I-V* characteristic curves under different irradiance levels, and the optimal switching surface (dashed line) [18], S(v,i)=0

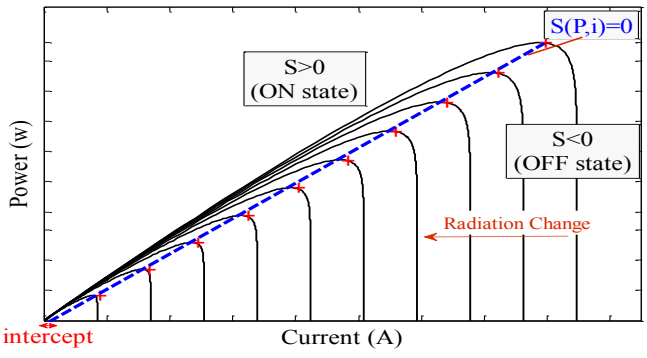

Fig. 2. *P-I* characteristic curves under different irradiance levels, and the proposed optimal switching surface (dashed line), S(P,i)=0

TABLE I. ANALYSIS RESULTS OF 230W RENESOLA PANEL

RENESOLA **230W** **POLYCRYSTALLINE** PANEL	**Electrical Characteristics (STC)** Maximum Power (P_{max})= 230 (W) Maximum Power Current (I_{mp})= 7.88 (A) Maximum Power Voltage (V_{mp})= 29.2(V) Temperature Coefficient of V_{OC}= - 0.3%/°C Temperature Coefficient of I_{SC} = 0.04%/°C Temperature Coefficient of P_{max} = - 0.4%/°C

Surface obtained using MSE: S_1= P-29.3215 (1-0.004 (T-25)) i+3.161=0 **Surface which links the origin to the MPP under STC:** S_2 =P-29.25 (1-0.004(T-25)) i=0	**Simulation Condition:** Irradiance varies from 1000(w/m2) to 50(w/m2) Temperature varies (5℃ to 65℃)

Radiation (w/m2)	I_{mpp}	P_{mpp}	$P_{mpp,1}$	$Error_1$	$P_{mpp,2}$	$Error_2$
1000	7.865	230.1	227.4	1.145	230.0	0.015
900	7.102	205.3	205.1	0.121	207.7	-1.170
800	6.28	181.0	180.9	-0.014	183.7	-1.513
700	5.479	156.9	157.5	-0.364	160.3	-2.129
600	4.71	133.3	134.9	-1.255	137.8	-3.374
500	3.915	110.0	111.6	-1.487	114.5	-4.107
400	3.131	87.1	88.6	-1.770	91.6	-5.143
300	2.339	64.6	65.4	-1.266	68.4	-5.901
200	1.557	42.6	42.5	0.075	45.5	-7.097
100	0.779	20.9	19.7	5.819	22.8	-9.032
50	0.387	10.3	8.1	20.679	11.3	-9.687

Temp(°c)	I_{mpp}	P_{mpp}	$P_{mpp,1}$	$Error_1$	$P_{mpp,2}$	$Error_2$
65	7.898	199	191.3	3.825	194.1	2.474
55	7.891	206.8	200.4	3.079	203.1	1.791
45	7.898	214.6	209.9	2.204	212.5	0.973
35	7.866	222.4	218.2	1.848	220.9	0.669
25	7.865	230.1	227.5	1.145	230.1	0.015
15	7.862	237.8	236.6	0.488	239.2	-0.593
5	7.863	245.4	245.8	-0.190	248.4	-1.231

Neglecting the intercept leads to more simplicity in the design procedure. In the other hand, considering columns E_{rror1} and E_{rror2} in the Table I, indicate that both surfaces S_1 and S_2 satisfy MPPT, so in the proposed algorithm the intercept is ignored. Thereby, under STC, k_1 can be calculated as follows:

$$K_1 = K_{STC} = \frac{P_{\max}}{I_{MPP}} \tag{5}$$

Where P_{max} and I_{MPP} are maximum power and the corresponding current respectively, under STC.

Temperature is the second parameter that causes characteristic curves of PVG's to vary. Fig. 3, demonstrates the impact of temperature variation on the PV *P-I* curve. As shown in this figure, for a given radiation, the current component of maximum power point is independent of temperature, with a good approximation, i.e. one can consider that MPP's in *P-I* curve due to temperature changes, are located on a vertical line. Considering this, the distance ΔP in Fig. 3, can be calculated by:

$$\Delta P = \gamma \Delta T \tag{6}$$

Consequently, the power at new MPP can be calculated as follows:

$$P_{MPP,new} = P_{\max} - \gamma \Delta T \; P_{\max} \tag{7}$$

Where $P_{MPP,new}$ is the power at new MPP, P_{max} is the maximum power under STC, γ is temperature coefficient of P_{max}, and ΔT is the difference between the temperature of the new condition and STC.

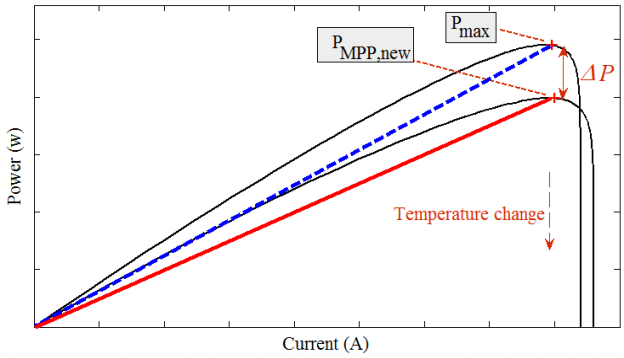

Fig. 3. PVG characteristic under different temperature levels. The dashed line is the optimal switching surface under STC, and the bold line is the optimal switching surface under a different temperature

Combining (5) and (7) yields to:

$$P_{MPP,new} = K_{STC}(1-\gamma \Delta T) I_{MPP} \tag{8}$$

Considering the above equations, this paper proposes a new switching surface which satisfies MPPT regarding irradiance and temperature simultaneously; the surface is defined as below:

$$S = P - K_{STC}(1-\gamma \Delta T) i = 0 \tag{9}$$

The blue dashed line in Fig. 2, shows the proposed switching surface.

Considering Fig. 2, Fig. 4, Fig. 5, and (9), working principle of the proposed method can be explained as below:

$$\begin{aligned} &S > 0 : \text{ON state} \\ &S < 0 : \text{OFF state} \end{aligned} \tag{10}$$

When switching surface S > 0, the main switches S_{m1} and S_{m2} are ON, and the magnetizing inductance L_m charges. So, the current *i* increases, and *S(P, i)* decreases. When S < 0, the main switches S_{m1} and S_{m2} are OFF, and the energy stored in magnetizing inductance flows to the load; consequently, *S(P,i)* increases. So, *S(P, i)* is kept in a switching band around *S(P,i)=0*. Hence, this controller constricts system's operation to the sliding switching surface.

III. THE PROPOSED LINEAR VSC METHOD

The block diagram of the proposed controller is shown in Fig. 4. It is named "linear and variable structure control" (LVSC) and consists of a sliding-mode controller that operates in parallel with a linear one [22]. This controller is a generalized and flexible scheme which takes advantage of the best features of linear control, smooth operation, and of VSC, robustness to perturbations and modeling uncertainties.

With the proposed system, the MPPT algorithm unit provides the sliding mode inner controller with an adaptive reference, which results in an adaptive switching surface. The inner feedback regulates a linear combination of the PVG power and current to attain its operation along a line in close vicinity to the MPP loci (see Fig. 2). This is accomplished in a rapid manner. Obviously, MPPT would be satisfied if *S(P, i)*

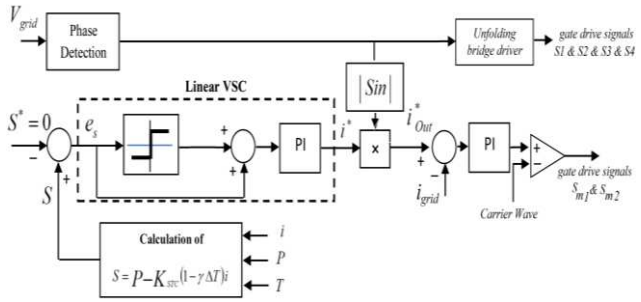

Fig. 4. Linear variable structure control (LVSC) block diagram for fast and robust tracking of MPP

can be maintained in zero value, as shown in Fig. 2.

The controller produces the reference output current i^* as given by:

$$i^* = \left(K_P + K_I / s\right)\left(e_s + K\,\mathrm{sgn}(e_s)\right) \tag{11}$$

Where K_I and K_P are the PI controller gains, K is the VSC gain, e_s is the error signal and *sgn* represents the sign function. The LVSC employs a switching component and a linear one. During transients, $e_s > K\ \mathrm{sgn}(e_s)$, and the linear (PI specific) behavior is dominant. In the steady-state, error is very small and the switching (VSC specific) behavior prevails and the ripple magnitude depends on the K gain. Adequate balance between linear and switching behavior is easily achieved by proper gain selection. PI gains are selected so that the linear control provides the desired dynamic response, while the VSC gain determines the robustness in steady-state operation.

IV. SYSTEM STRUCTURE AND ANALYSIS OF THE POROPOSED TWO-SWITCH FLYBACK MICRO INVERTER

In PV ac module systems, the flyback inverter is an attractive solution as the single-phase grid connected inverter because of the advantages of fewer components, simplicity, and isolation between the PV modules and the grid line [23].

The proposed micro inverter topology is shown in fig. 5. It is comprised of a two switch flyback converter, unfolding bridge, and C-L filter. S_{m1} and S_{m2} are the main power switches. D_1 and D_2 are the calmping diodes; D_3 is rectifier diode. N_p and N_s are the primary and secondary windings respectively. S_1-S_4 form the CSI to unfold the rectified sinusoidal waveform to the grid. L_{l1} is the leakage inductance

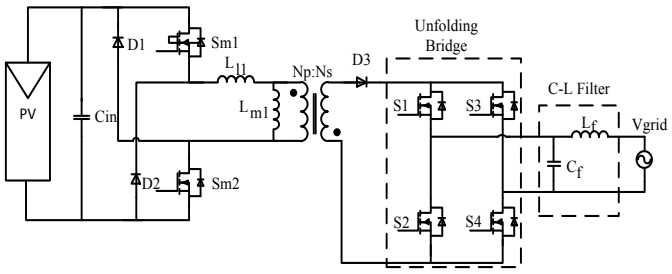

Fig. 5. The proposed micro inverter topology

, and L_m is the magnetizing inductance of the transformer.

A. Design procedure

Reference [24] indicates that in power ranges under 200 watts DCM control strategy achieves higher efficiency over boundary conduction mode (BCM). Moreover, DCM is easier in the case of control strategy.

It is noticed that the output power p_{out} *(t)* during a half line period is a pulsating power following a squared sine wave given by:

$$P_{out}(t) = 2P_0 \sin^2(\omega t) \tag{12}$$

Where P_0 is the average output power. Fig. 4, shows the control block diagram. The phase detection block detects the phase angle, amplitude, and frequency of grid voltage in order to make switching signals of unfolding bridge and the reference signal of main power switches. Using PV power and current, switching surface is calculated and then an error is defined as:

$$e_s = S - S^* \tag{13}$$

Where S is the switching surface and S^* is the reference. Sliding-plus-PI controller uses e_s signal as input and generates a reference signal i^*. Using i^* and phase detection block, the reference current i^*_{Out} is finally adjusted as [24]:

$$i^*_{Out} = 2\sin(\omega t)\sqrt{\frac{P_0}{L_p f_s}} \tag{14}$$

A. Parameter design

In the case of selecting turns ratio, there is a limitation as follows:

$$nV_m \langle V_{in} \tag{15}$$

Where V_m is the maximum output voltage, V_{in} is the input voltage, and n is turns ratio. This limit is considered, in order to prevent the conduction of D_1 and D_2 and transferring the energy stored in L_m to the source, when main switches S_{m1} and S_{m2} are OFF.

In order to reassure the micro inverter will always operate under DCM, the following limitation should be taken into account [24]:

$$d_{\max} \le 0.5 \tag{16}$$

Where the maximum duty cycle is defined as below:

$$d_{\max} \le \left(1 + \frac{V_{in}}{nV_m}\right)^{-1} \tag{17}$$

The specifications are as follow: input voltage (MPP): V_{in}=50 V; grid voltage: *Vgrid* = 220 VAC; grid frequency: f_{grid} =50 Hz; switching frequency: f_s =100 kHz;

Considering the above specification, turns ratio must be smaller than 0.16. The average primary current is [24]:

$$I_{P,avg} = \frac{1}{4}\frac{V_{in} T_s d_{\max}^2}{L_m} \quad (18)$$

Where T_s is the switching time interval, and L_m is the magnetizing inductance. The input power is defined as below:

$$P_{Pv} = 2 V_{in} I_{P,avg} = \frac{1}{2}\frac{V_{in}^2 T_s d_{\max}^2}{L_m} \quad (19)$$

For P_{PV}=200 W, V_{in}=50 V and d_{max}=0.38, the maximum transformer primary inductance $L_{P,max}$=9 µH; considering L_P=*0.8* $L_{P,max}$=*7.2* µH.

The input electrolyte capacitor C_{in} is used to compensate the unbalance of constant output power of PV and pulsating power transferred to the grid. So, the value of input capacitor is determined by the energy has to be stored in it, according to [24] the size of this capacitor is:

$$C_{in} = \frac{P_{pv}}{\omega V_{in} \Delta V} \quad (20)$$

Where ω is the angle frequency of grid voltage, and ΔV is the maximum peak to peak ripple voltage of input capacitor. To limit ΔV to two volts, the required capacitance is:

$$C_{in} = 6.4\ mF \quad (21)$$

V. Simulation Results

In order to verify the dynamic response, stability and high efficiency of the proposed MPPT method, as well as the theoretical analysis of the proposed micro inverter topology, a simulation platform based on PSIM 9.0 software integrated with MATLAB is established. Table II presents the detailed specifications of the simulation platform.

TABLE II. Parameters of Simulation

Parameter	*Symbol*	*Value*	*Unit*
Grid frequency	f_{grid}	50	Hz
Switching frequency	f_s	100	kHz
Transformer turn ratio	*Np / Ns*	0.1	
Input capacitance	C_{in}	6.4	mF
Output filter capacitance	C_f	0.3	µF
Output filter inductance	L_f	6.1	mH
Magnitizing inductance	L_m	7.32	µH
Leakage inductance	L_l	0.1	µH
PV module maximum power	P_{max}	200	W
PV module voltage at P_{max}	V_{mpp}	50	V
PV module current at P_{max}	I_{mpp}	4	A
Temperature coefficient of V_{oc}	β	-0.3	%/°C
Temperature coefficient of I_{sc}	α	0.04	%/°C
Temperature coefficient of P_{max}	γ	-0.4	%/°C

A. Simulation results

In Fig. 6, the output current i_{out}, and the sample of the grid voltage are shown in full load condition. The amplitude of i_{out} is 1.28 ampere and it is in phase with the grid voltage which meets the design requirements.

In order to show the system dynamic performance under extreme step changes in irradiance and temperature, the below simulation results are presented.

Fig. 7 shows the system performance under an extreme step change in irradiance. Irradiance decreases from 1000 (w/m^2) to 600 (w/m^2), and the ambient temperature is 25°C. The MPPT algorithm converges within 0.2 second and the amplitude of the fluctuations during steady-state is very small (Fig. 7(b)). Therefore, in the case of even big changes in irradiance, the proposed MPPT algorithm satisfies both fast response and low steady-state fluctuations.

Fig. 8 shows the system performance under extreme step changes in temperature. In this scenario irradiance is 1000 (w/m^2), and temperature increases from 25°C to 55°C. Regarding the output PVG power shown in Fig. 8(a) the MPPT algorithm converges within 0.1 second which verifies fast response. Moreover, the small amplitude of the error signal which is shown in Fig. 8(b) verifies low steady-state fluctuations in the case of temperature changes.

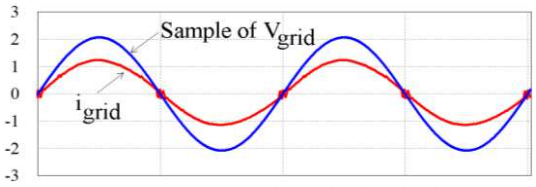

Fig. 6 Output current and sample of grid voltage

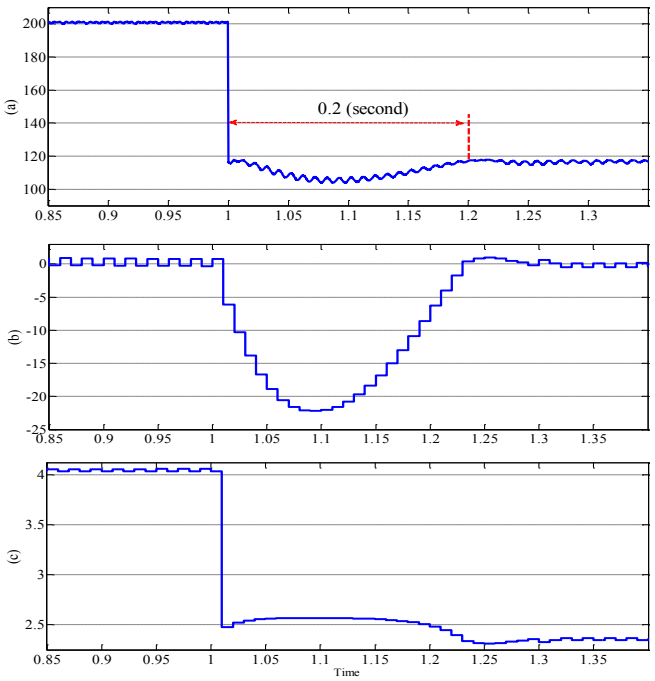

Fig. 7. System performance under step change in irradiance, (a) PV output power, (b) error signal, and (c) PV output current

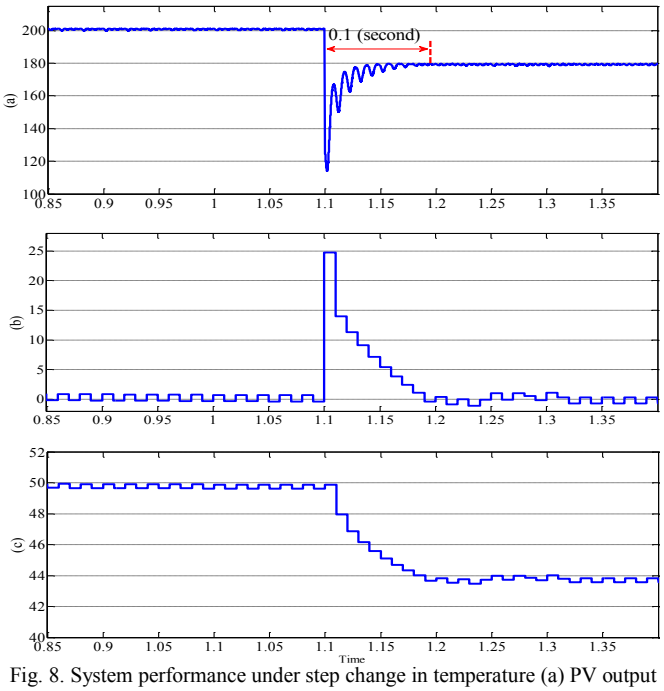

Fig. 8. System performance under step change in temperature (a) PV output power, (b) error signal, and(c) PV output voltage

VI. CONCLUSION

In this paper a sliding mode based MPPT was presented with introducing a novel switching surface. The proposed surface is based on *P-I* characteristics of PV panels dependent on both radiation and temperature, simultaneously. Moreover, a linear variable structure controller was employed to reduce the output power fluctuations during steady-state behavior while the fast response and robustness merits of the sliding mode controller were preserved. The performance of this fast and robust MPPT employing sliding mode was verified using some simulation results of a grid-tied two switch flyback micro inverter.

References

[1] M. A. Eltawi and Z. Zhao, "MPPT techniques for photovoltaic applications," ELSEVIER renewable and sustainable energy reviews 25, pp. 793-813, 2013.

[2] K. H. Hussein, I. Muta, T. Hoshima, and M. oskada, "Maximum photovoltaic power tracking: An algorithm for rapidly changing atmospheric conditions," in IEEE Proc. Gener., Transm., Distrib., 1995, vol. 142, pp. 59-64.

[3] Z. Zinger and A. Braunstein, " Dynamic matching of a Solar-Electriacl(photovoltaic) system an estimation of the minimum requirements on the matching system," IEEE Trans. Power App. Syst., vol. PAS-100, no. 3, pp. 1189-1192, 1981.

[4] T. Esram and P. L. Chapman, " Comparison of photovoltaic array maximum power point tracking techniques," IEEE Trans. Energy Convers., vol. 22, no. 2, pp. 439-449, June. 2007.

[5] D. Shmilovitz, "On the control of photovoltaic maximum power point tracker via output parameter," IEEE Trans. Power Appl., vol. 152, no. 2, pp. 239-248, Mar. 2005.

[6] S. Jain and V. Agarwal, "A new algorithm for rapid tracking of approximate maximum power point in photovoltaic systems," IEEE Power Electron. Lett., vol. 2, no. , pp. 16-19, Mar. 2004.

[7] L. Gao, R. A. Dougal, S. Liu, and A. Lotova, "Portable solar systems using a step-up power converter with a fast- speed MPPT and a parallel configured solar panel to address rapidly changing illumination," in Proc. IEEE APEC, Anaheim, CA, Mar. 2007, pp. 520-523.

[8] L. Gao, R. A. Dougal, S. Liu, and A. Lotova, "Parallel-Connected solar PV system to address partial and rapidly fluctuating shadow conditions," IEEE Trans. Ind . Ellectron., vol. 56, no. 5, pp. 1548-1566, May 2009.

[9] M. Sokolov et al., "Small-signal model of photovoltaic power converter for selection of perturb and observe algorithm step time," in Proc. 14th Eur. Conf. Power Electron. Appl. (EPE), Sep. 2011, pp. 1-6.

[10] R. F. Coelho, F. M .Concer, and D. C. Martins, "Analytical and exprimental analysis of DC-DC converters in photovoltaic maximum power point tracking applications," in Proc. 36th Annu. Conf. IEEE Ind. Electron. Soc. (IECON), Nov. 2010, pp. 2778-2783.

[11] V. V. R .Scarpa, G. Spiazzi, and S. Buso, "Low complexity MPPT technique expliting the effect of the PV cell series resistance," IEEE Trans. Ind . Electron., vol. 56, no. 5, pp. 1531-1538, May 2008.

[12] M. Sokolov and D. Shmilovitz, "A modified MPPT scheme for accelerated convergence," IEEE Trans. Energy Convers., vol. 23, pp. 1105-1107, Dec. 2008.

[13] J. Leppaaho and T. Suntio, "Dynamic properties of PCM-controlled current-fed boost converter in photovoltaic system interfacing," in Proc. 14th Eur. Conf. power Electron. Appl. (EPE), Sep. 2011, pp. 1-10.

[14] S. Singer, R. Giral, J. Calvente, R. leyva, L. Martinez-Salamero, and D. Naunin, "Maximum power point tracker based on a loss free resistor topology," in Proc. Fifth Eur Eur. Space Power Conf. (ESPC), Tarragona, Spain, Sep. 21-25, 1998.

[15] D. Sera, R. Teodorsecu, G. Hantschel, and M. Knoll, "Optimized maximum power point tracker for fast-changing environmental conditions," IEEE Trans. Ind. Electron., vol. 55, pp. 2629-2637, 2008.

[16] G. Spiazzi et al., "Application of sliding mode control to switched-mode power supplies," G. Circuits, Syst. Comput. (JCSC), vol. 5, no. 3, pp. 337-354, Sep. 1995.

[17] L. Martinez-Salamero et al., "Why is sliding mode control methodology needed for power converters," in Proc. 14th Int. Power Electron. Motion Control Conf. (EPE/PECM), 2010, pp. S9-25-S9-31.

[18] Y. Levron and D. Shmilovitz, "Maximum power point tracking employing sliding mode control," IEEE Trans. Circuits and Syst., vol. 60, no. 3, Regular Papers , Mar. 2013.

[19] S. B. Kjaer, and F. Blaabjerg, "Design optimization of a single phase inverter for photovoltaic applications," IEEE. 34th Annu. Power Ellectron. Specialist Conf. 2003.

[20] Y. Konoshi, Y. Huang, and M. Hsieh., "Utility interface high-frequency flyback transformer link three-phase inveter for photovoltaic ac module," IEEE 35th Annu. Conf. Ind. Electron., 2009.

[21] K. Ding, X. Bian, H. Liu, and T. Peng, "A matlab –simulink based pv module model and its application under conditions of nonuniform irradiance," IEEE Trans. Energy Con., vol. 27, no. 4, pp. 864-872, 2012.

[22] C. Lascu, I. Boldea and F. Blaabjerg, "very Low Speed Variable structure control of sensorless induction machine drives without signal injection", ", IEEE Trans. Ind. Appl., vol. 41, No. 2, Mar./Apr. 2005, pp. 591-598.

[23] D. M. Beller, "Hard-switching and soft-switching two switch flyback PWM dc-dc converters and winding loss due to harmonics in HF transformers," Ph.D. dissertation, Wright state university, 2010.

[24] Z. Zhang, X. He, and Y. Liu, "An optimal control method for photovoltaic grid-tied interleaved flyback micro-inverters to achieve high efficiency in wide load range," IEEE Trans. Power Electron., vol. 28, pp. 5074-5087, 2013.